ORIGINAL ARTICLE

CLINICAL ORAL IMPLANTS RESEARCH **WILEY**

Comparative osseointegration of hydrophobic tissue-level tapered implants—A preclinical in vivo study

Jean-Claude Imber[1] | Azita Khandanpour[1] | Andrea Roccuzzo[1] | Delia R. Irani[1] | Dieter D. Bosshardt[1] | Anton Sculean[1] | Benjamin E. Pippenger[1,2]

[1]Department of Periodontology, School of Dental Medicine, University of Bern, Bern, Switzerland

[2]Department of Preclinical Research, Institut Straumann AG, Basel, Switzerland

Correspondence
Benjamin E. Pippenger, Department of Periodontology, School of Dental Medicine, University of Bern, Freiburgstrasse 7, Bern CH-3010, Switzerland.
Email: benjamin.pippenger@unibe.ch

Funding information
Institut Straumann AG

Abstract

Purpose: To histometrically compare the osseointegration and crestal bone healing of a novel tapered, self-cutting tissue-level test implant with a standard tissue-level control implant in a submerged healing regimen.

Materials and Methods: In a mandibular minipig model, implants were inserted and evaluated histometrically after a healing period of 3, 6, and 12 weeks. The primary outcome was the evaluation of bone-to-implant contact (BIC) and secondary outcomes were primary stability as per insertion torque and first BIC (fBIC). Outcomes for the test and control implants were compared using Wilcoxon signed-rank tests and mixed linear regression models.

Results: Insertion torque values were significantly higher for the test (50.0 ± 26.4 Ncm) compared to the control implants (35.2 ± 19.7 Ncm, $p = .0071$). BIC values of test implants were non-inferior to those of control implants over the investigated study period. After 12 weeks, the corresponding values measured were $81.62 \pm 11.12\%$ and $90.41 \pm 4.81\%$ ($p = .1763$) for test and control implants, respectively. Similarly, no statistical difference was found for fBIC values, except for the 12 weeks outcome that showed statistically lower values for the test (-675.58 ± 590.88 μm) compared to control implants (-182.75 ± 197.40 μm, $p = .0068$).

Conclusions: Novel self-cutting tissue-level implants demonstrated noninferior osseointegration and crestal bone height maintenance to the tissue-level implants. Histometric outcomes between both implants demonstrated test implants were statistically noninferior to control implants, despite substantial differences in the bone engagement mechanism and resulting differences in insertion torque and qualitative bone healing patterns.

KEYWORDS
crestal bone formation, implant geometry, osseointegration

1 | INTRODUCTION

The tissue-level implant represents a clinically well-established concept of prevailing relevance and validity (Buser et al., 2004; Cochran, 2000; Duong et al., 2022; Insua et al., 2023). Its ongoing popularity is driven by distinct advantages comprising a reduced number of required surgical interventions along with a documented ability to promote crestal bone stability and long-term survival (Cosola et al., 2020; Kim et al., 2018). Part of these characteristics has been associated with the supracrestal location of the implant-abutment interface. This feature has been reported to reduce the

microbiologically related inflammatory stimulus and abutment-implant micromovement-associated mechanical stresses acting on the crestal bone, causing it to recede (Cochran, 2000; Hermann et al., 2001; Sasada & Cochran, 2017). Corresponding implants with microrough, sandblasted and acid-etched (SLA) surfaces have been reported to show a 10-year survival rate of as high as 99.7% (van Velzen et al., 2015) and up to 93% after 20-year of loading (Roccuzzo et al., 2022).

Driven by advancements in technology and clinical science, implant dentistry has steadily witnessed a significant shift towards early and immediate procedures (Chen et al., 2004; Schulte et al., 1978). Technical progress in implant design, surgical workflows, and refined case selection have rendered this placement modality clinically, biologically, and esthetically successful (Bilhan et al., 2010; Kan et al., 2018; Tettamanti et al., 2017; Wilson et al., 2016; Xu et al., 2016). The increasing trend towards immediate procedures has reemphasized the critical role of primary stability as a key factor for implant osseointegration (Javed et al., 2013).

Primary stability is affected by multiple factors, comprising bone density, surgical technique, and implant design (Emmert et al., 2021; Imai et al., 2022; Javed et al., 2013; Molly, 2006; Romanos et al., 2014). Recently, novel tapered design concepts for high primary stability have been introduced (El Chaar et al., 2021; Francisco et al., 2021; Hadaya et al., 2022). A characteristic feature of this design concept is related to a self-cutting geometry with characteristic protruding threads of coronally progressing thickness. In vitro-studies have shown that the described novel implant type results in high primary stabilities through apical engagement in cortical bone irrespective of the used host bone quality (Emmert et al., 2021; Ibrahim et al., 2020).

El Chaar et al. (2021) have recently presented a tissue-level variant of this novel implant design concept and compared its osseointegrative potential with long-term established tissue-level implants in a moderate-dense bone situation. Despite the differences in placement and host bone interaction of the corresponding hydrophilic microrough functionalized implant variants, the authors reported equivalent histometric outcomes related to osseointegration and crestal bone formation. Very recently, another possible variation of this novel design with a conventional SLA surface has been developed, raising the question whether noninferior outcomes between novel and established tissue-level implants can be obtained. The aim of this preclinical study was to histologically and histometrically evaluate the two implant geometries, i.e. novel self-cutting tapered test implants and the established tissue-level implants, compare in terms of osseointegration and crestal bone healing when the implants are functionalized with a conventional SLA surface and implanted in cortical hard bone.

2 | MATERIALS AND METHODS

2.1 | Study design

This longitudinal, nonrandomized controlled preclinical study has histometrically compared the osseointegration and crestal bone healing and apposition of two types of tissue-level implants, i.e.

conventional, long-term established control tissue-level implants (Straumann® TL, Standard Plus [SP] RN Ø4.1×8 mm, Roxolid®, SLA®, Institut Straumann AG, Basel, Switzerland) and novel test tissue-level implants with a tapered, self-cutting and characteristic protruding thread endosteal geometry (Straumann® TLX, SP RT Ø3.75×8 mm, Roxolid®, SLA®) as part of a submerged healing regimen (Figure 1). Both implants were produced from Roxolid® (TiZr alloy). The endosteal parts of both implants were micro-roughened by sandblasting and acid etching (SLA). Both implant types were implanted according to the manufacturer's instructions.

A total of 64 implants (10 implants per group and time point; 2 implants per group in a backup animal carried over throughout the study) were inserted in a healed, mandibular minipig model and subjected to qualitative histological and quantitative histometric analysis after a healing time of 3, 6 and 12 weeks, respectively (the experimental unit was 1 minipig in this study). The primary outcome variable of this study is the bone-to-implant contact (BIC). The sample size was determined based on previous animal studies with similar readouts in which a sample size calculation determined a minimum of $n = 6$ was necessary; this study aimed at a minimum of $n = 9$ to adhere to the ISO10993-6 which details the minimum number of samples per group for a medical device study. The study design including preparation and use of the animal model and corresponding time points of interventions are schematically illustrated in Figure S1.

The study was conducted at the Biomedical Department of Lund University, Lund, Sweden, and approved by the local ethics committee (approval number 2021-15-0201-00876). It respected the Swedish Animal Protection Law, adhered to the ARRIVE Guidelines, and was designed and performed under consideration of the 3R (Replace, Reduce, Refine) guidelines for animal experimentation. The proper institutional and national guidelines have been followed for the care and use of the animals in the study.
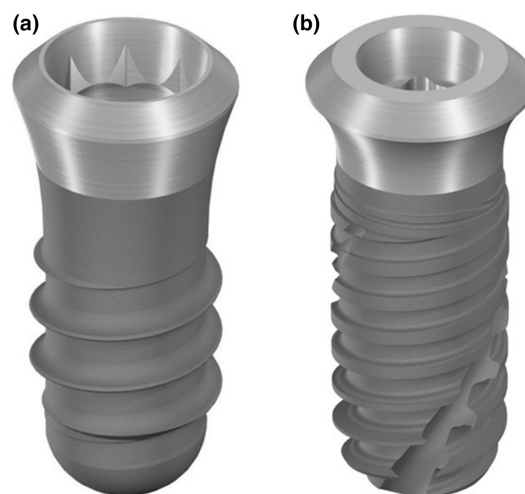
FIGURE 1 Side-by-side comparison of control, established Tissue-Level (TL) implants (a) and novel tapered, self-cutting Tissue-Level Tapered (TLX) test implants (b).

2.2 | Animal model

Thirteen female Ellegaard Goettingen Minipigs (A/S, Dalmose, Denmark) aged between 20 and 23 months and with a body weight of 31–50 kg were used. The study design included 4 animals per time point and one additional animal to compensate for possible dropouts. The animals were housed in standard boxes in groups of 3 and provided a standard diet (soft food) expanded for Minipigs (SDS Standard Service, U.K. #801586). Housing started at least 10 days before intervention to adapt the animal to the experimental environment. All animals were fasted overnight before surgeries to prevent postoperative emesis.

2.3 | Detailed study design and site and animal-specific group allocation

The animal and implantation site allocation per animal was defined prior to surgery and is illustrated in Figure S2. Specifically, five implant positions and 10 implants were defined per hemi-mandible and animal, respectively. Consecutive animals received in an alternating scheme from one animal to the next four anterior and six posterior implants, divided into two or three test and two or three control implants per hemi-mandible, positioned in a contralateral configuration. Complementary implant positions were used for another implant study setup of a comparable setup. Test and control groups were switched between the right and left side and between anterior and posterior implant positions, respectively, from one animal to the next to ensure equal distribution of the experimental groups over mandible sides (Figure S2).

2.4 | Anaesthesia and veterinary care

All surgical interventions were carried out under general anaesthesia. Before the surgery, an intramuscular injection of Streptocillin (0.1 mL/kg) was given. Anaesthesia was induced with intra-muscular injection of Zoletil mixture XKB* (0.1 mL/kg). After intubation, the animals received Atropine (1 mg/mL, at a dose of 0.04 mL/kg, I.M.), Metacam (20 mg/mL, at a dose of 0.02 mL/kg, I.V.) and propofol (10 mg/mL, at a dose of 0.1–0.2 mL/kg) to maintain anaesthesia. Before starting the surgical interventions, local anaesthesia was administered with a mixture of Xylopin + noradrenalin (20 mg/mL + 12.5 μg/mL, at 1.8 mL per hemi-mandible).

During the surgery, the animals received an I.V. access with a flow rate of 2 mL/kg/h (saline solution). Propofol administration was continuously reduced in the course of surgery as per the following regimen: Induction: Bolus of 0.5 mg/kg, 3–15 min: 8 mg/kg/h, 15–40 min: 6.5 mg/kg/h, 40–200 min: 5.5 mg/kg/h, 200+ min: 4.5 mg/kg/h.

Post-operation, the animals received Vetergesic (0.3 mg/mL, at a dose of 0.1 mL/kg, I.V./I.M.) 4 h after the surgery. They also received Cerenia (0.1 mL/kg, I.V/I.M) if needed. During the first day post-surgery, animals received Vetergesic (0.3 mg/mL, at a dose of 0.1 mL/kg, I.V/I.M) if necessary. All animals received an oral suspension of Streptocillin (0.1 mL/kg, I.M). and until day 2 post-surgery and Metacam (15 mg/mL, at a dose of 0.03 mL/kg) until day 5 post-surgery.

During anaesthesia, the animals were intubated and breathing withheld by a ventilator. Vital parameters were monitored continuously (pulse oximetry, rectal temperature, blood pressure, CO_2).

All anaesthetics, analgesics, and other medications were administered in doses and intervals following standard veterinary practice and according to the study objectives.

2.5 | Tooth extraction

Test sites were prepared by careful bilateral extraction of mandibular premolars (P2–P4) and first mandibular molars (M1) under general anaesthesia via a minimally invasive surgical approach, i.e. without raising a flap. Extraction sites were allowed to heal for 12 weeks before the placement of implants (Figure S1).

2.6 | Osteotomy preparation, implant placement, primary stability, and healing

Test and control implants were placed using the procedure illustrated in Figure 2. In brief, Implant placement was performed sequentially per hemi-mandible and started by exposing the mandibular alveolar ridges by mid-crestal incision and reflection of a mucoperiosteal flap. The alveolar ridge was carefully flattened using a cylindrical cutting bur. Implant osteotomies for the test and control implants were prepared freehand according to the manufacturer's instructions, if applicable to the implant line corresponding protocols for hard bone.

Control implant osteotomies were prepared using the TL set (Institut Straumann AG, Switzerland), involving pilot drilling using needle drills and extending the osteotomy diameter using sequential drilling with Ø2.2, Ø2.8, and Ø3.5 mm drills. Osteotomy depth and orientation were verified using corresponding alignment pins. Control implant osteotomies were finalized using Ø4.1 mm profile and Tap drills. Test implant osteotomies were prepared following a hard bone protocol using Velodrill sets (Institut Straumann AG, Switzerland), employing pilot drilling (Ø 2.2 mm), followed by Ø2.8 mm and Ø3.5 mm drilling to the final depths. The coronal 4 mm of the osteotomy was widened using a Ø3.7 mm drill. All drilling procedures were performed under constant irrigation. Profile drilling (TLX, RT Profile Drill, short, for implants Ø 3.75) was employed to prepare the osteotomy for subcrestal smooth to microrough surface margin placement.

Test and control implants were placed 1 mm subcrestally at 15 rpm using a motorized handpiece. Insertion torques (primary stability) were measured using a specialized, high precision manual torque wrench specifically developed for preclinical applications (Institut Straumann AG, Basel, Switzerland). Implants were
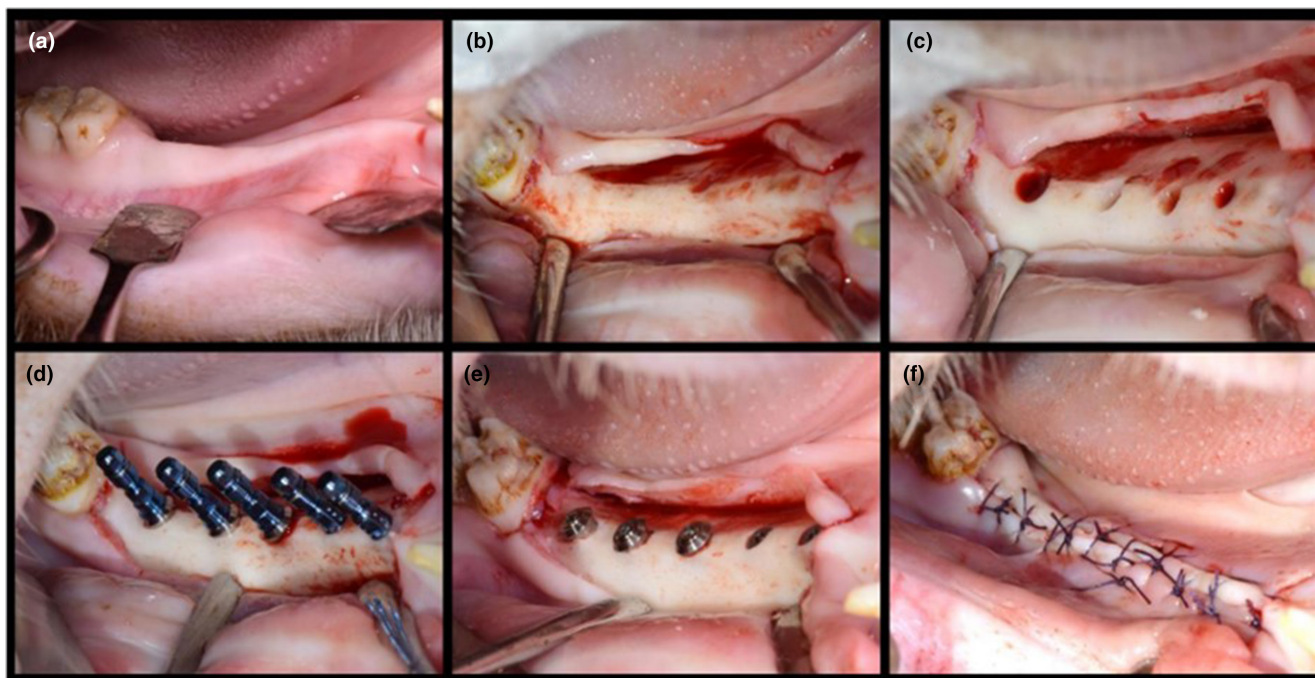
FIGURE 2 Illustration of the surgical procedure. (a) Lateral view of the exposed healed mandibular ridge prior to surgery. (b) Exposed mandibular implantation test site after mucoperiosteal flap elevation and alveolar bone crest flatting. (c) Implantation sites after osteotomy preparation. (d) Situation after implant placement with transfer pieces in place. Five implants were placed per hemi-mandible, (e) Situation after installation of healing caps and (f) after primary wound closure and suturing for submerged healing. Test implants were placed in the three distal positions; the two mesial positions were used for another implantation study.

subsequently equipped with implant closure caps (Titanium TLX implant closure caps and Tissue-Level RN Closure caps, height 0 mm, respectively) before primary wound closure of wound margins for submerged healing using resorbable sutures (Vicryl 4–0).

Antibiotic cover was administered until 3 days post-surgery (pen&strep, Norbrook, UK, 1 mL/10 kg i. m). Analgesics were administered if considered necessary, as described above.

2.7 | Euthanasia

Four animals each were euthanized 3 and 6 weeks after surgery, respectively. Five animals were euthanized after 12 weeks. An intracardiac arrest was induced by injecting a 20% pentobarbital solution (Euthanimal 400 mg/mL, Pentobarbitalnatrium, Alfasan Nederland B.V., the Netherlands).

Block sections of the mandibular implantation sites were obtained using an oscillating autopsy and preserving the soft tissues. Sections were fixed in formalin (4% formaldehyde solution) for at least 2 weeks before histological processing.

2.8 | Histological processing

Histological processing was performed as previously described (Parvini et al., 2023). Briefly, block sections were immersed in formalin buffer solution, dehydrated using ascending grades of alcohol and xylene,

and subsequently infiltrated and embedded in methyl methacrylate for nondecalcified sectioning. Buccolingual sections of 200 μm were prepared by cutting and grinding. The resulting sections were stained with toluidine blue and basic fuchsin for histometric evaluation.

2.9 | Qualitative histology and quantitative histometry

The relevant aspects related to the histomorphometric evaluation are illustrated in Figure 3. Histomorphometric parameters were evaluated on central mesiodistal sections of the implant. Histomorphometric parameters comprised the BIC as defined by the relative percentage of the perimeter of the endosteal microrough part of the implant in contact with Bone (Figure 3b) and the first BIC (fBIC) as defined by the distance between the machined to microrough endosteal surface margin to the most apical level of crestal bone in contact with the implant surface (Figure 3c). The fBIC values were reported as average values derived from the mesial and distal aspects allowing positive and negative values resulting from crestal bone levels lying more coronal or apical regarding the reference margin of the implant, respectively.

2.10 | Statistical evaluation

BIC and fBIC outcomes were summarized as means, standard deviations, medians and interquartile ranges. BIC, fBIC and maximum

insertion torque (maxIT) between test and control samples were compared using the Wilcoxon signed-rank tests. The pairing was performed by the animal and mandibular position.

Adjusted comparisons and noninferiority tests were performed using a mixed linear regression model that adjusted for animal effect, side of the mandible and position of test and control implants. The animal effect was introduced in the model as a random effect. All other factors were set as fixed effects. A p-value of $<.05$ was considered statistically significant. For the hypothesis of noninferiority of the test device compared to a control device, the average effect and its two-tailed 90% confidence interval (equivalent to a one-tailed 95% confidence interval) were calculated. The lower confidence interval limit served as the tolerance range (T.R.) for supporting the null hypothesis. The detailed results of the mixed regression models and results relevant to the noninferiority testing are provided as part of the supplementary information in Tables S1–S3.

Noninferiority testing between test and control implants was performed based on the following null and alternative hypotheses (H_0 and H_1):

H0. Average BIC (test)—Average BIC (control) $\leq$ T.R.

H1. Average BIC (test)—Average BIC (control) $>$ T.R.

Noninferiority testing of fBIC between implants of specific subgroups was performed with the following null and alternative hypotheses (H_0 and H_1):

H0. Average fBIC (test) $\leq$ T.R.

H1. Average fBIC (test) $>$ T.R.

3 | RESULTS

The recovery from surgeries was uneventful in all animals. No specific surgical, perioperative, or postoperative complications were observed. There were no signs of inflammation during the healing period. The occurrence of one sample dropout during histological processing (unable to find cutting axis) rendered a sample unsuitable for histomorphometric evaluation. Additionally, while four animals per timepoint were used, one extra animal (implanted identically to the other animals) was included as a backup in case of animal dropouts during healing. This backup animal was carried forward after each termination if no animals had dropped out at that given termination time point. At the final timepoint, the animal was included in the final timepoint, resulting a higher n for the 12-weeks termination endpoint. Taken together, the final analyzed sample sizes per group and time point were $n = 10$ at 3 weeks healing for both groups, $n = 10$ and $n = 9$ at 6 weeks healing and for test and control groups, respectively, and $n = 12$ at 12 weeks for both groups (Tables 1 and 2).

3.1 | Qualitative histological characterization

The representative histological sections of test and control implants in Figure 4 illustrated the characteristic implant host-bone interaction and the associated peri-implant and crestal bone healing of the corresponding test and control implant geometries in their respective implant osteotomies. Specifically, control implants were characterized by a relatively close contact between the implant perimeter and osteotomy. Histological sections at early time points after 3 weeks of healing revealed the presence of small and narrow spaces between the implant surface and the
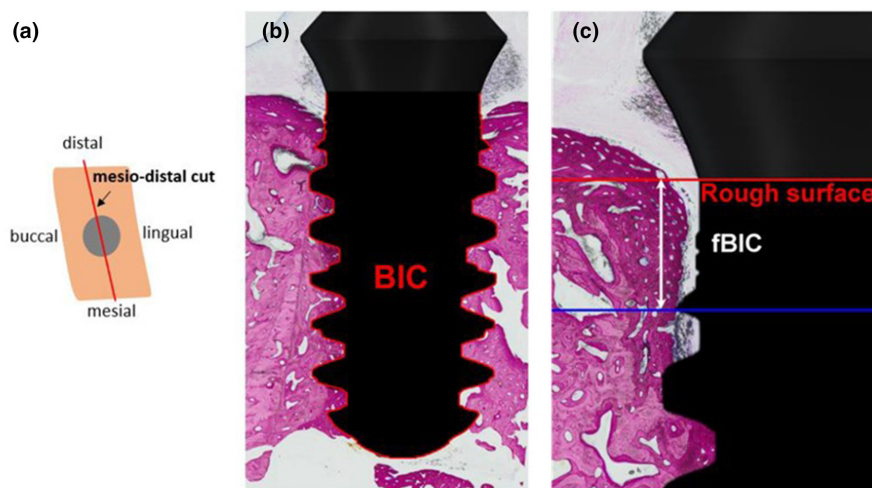
FIGURE 3 Illustration of the histometric parameters. (a) Illustration of the orientation of the histological axis in superior view. Histologic slices were prepared in a mesiodistal direction through the centre of the implants. (b) Bone-to-implant contact (BIC, red line) as the percentage of the implant perimeters endosteal microrough surface in contact with bone. (c) First bone-to-implant contact (fBIC) in the apical direction (white arrow) was measured from rough to machined surface interface (red line) to the most coronal aspect of bone in direct contact with the implant surface (blue line). Mesial and distal values were used to calculate reported averages (mesiodistal).

osteotomy walls (Figure 4a), which were consecutively occupied by newly formed bone with ongoing healing at later time points (Figure 4b,c). Intermediate time points after 6 weeks of healing evidenced the presence of newly formed bone, which could be distinguished from old bone by a relatively more pronounced staining in the histological longitudinal sections and an ongoing remodeling in close association with the implant surface (Figure 4b). Histological micrographs at late healing time points revealed a tight and complete osseointegration of control implants along the entire implant perimeter (Figure 4c).

Test implants exhibited a pronounced thread tip engagement with the vertical host-bone walls of the osteotomy in the central and apical implant aspects (Figure 4d). New bone formation at early healing time was most pronounced at the implant thread tips. The micrographs also revealed that the characteristic apical implant core tapering in conjunction with the vertical osteotomy walls resulted in inter-thread voids of apically increasing volume, which were specifically apparent at early time points (Figure 4d). These voids were observed to be progressively filled with newly formed bone with increasing healing time (Figure 4e,f). Late time points of test implants were again characterized by complete osseointegration and an intricate contact of newly formed bone along the entire implant perimeter (Figure 4f).

3.2 | Bone-to-implant contact

Figure 5 and Tables 1 and 3, as well as Tables S1–S3, compare the BIC values between test and control implants in the function of the study duration. They also provide the results of the statistical analysis and noninferiority tests conducted, respectively. Control implant osseointegration was characterized by a constant increase in BIC values from $71.08 \pm 22.18\%$ after 3 weeks to $80.97 \pm 9.40\%$ after 6 weeks and $90.41 \pm 4.81\%$ after 12 weeks, respectively. BIC of test implants, on the other hand, increased from $73.39 \pm 11.12\%$ after 3 weeks to $82.08 \pm 9.67\%$ after 6 weeks and remained steady, resulting in $81.62 \pm 11.12\%$ weeks after 12 weeks. Direct comparisons of average BIC values using Wilcoxon signed rank tests in Table 3 and corresponding linear regression model-adjusted outcomes in Table S1–S3 indicated that the BIC of test were noninferior to control implants for all tested time points. Adjusted average BIC of test implants were also consistently higher compared to the lower 95% confidence interval of control implants defined as the T.R. for the noninferiority testing. This outcome supported the alternative hypothesis of test implants being noninferior to control implants in terms of BIC at all studied time points.

3.3 | First bone-to-implant contact

Figure 6 illustrates the temporal evolution of mesiodistal fBIC values around test and control implants. Table 2 reports the corresponding fBIC values. Table 3 and Tables S1–S3 present direct and adjusted comparisons using linear regression models, respectively. The fBIC values of test implants were noninferior to control implants,

except for the 12-week healing time point with fBIC values around control implants ($-182.75 \pm 197.40 \mu m$) being higher than the ones of test implants ($-675.58 \pm 590.88 \mu m$, $p = .0068$). Linear regression-adjusted differences reached statistical significance at this time point ($p = .0119$).

At the 3 and 6-week time points, test implants were based on the adjusted comparisons noninferior to control implants. At the 12-week time point, the comparison failed to support the alternative hypothesis, suggesting higher fBIC values for the test compared to the control implants.

From a qualitative perspective, fBIC values around control implants tended to increase consistently over time. The corresponding values around the test implants remained stable at the 3 and 6-week time points and decreased at the later time point.

3.4 | Maximum insertion torque

Based on the averaged maxIT values depicted in Figure 7, both types of implants exhibited high levels of primary stability, above the manufacturer-indicated minimum thresholds. Test implants displayed significantly higher MaxIT values (50.0 ± 26.4 Ncm) compared to the control implants (35.2 ± 19.7 Ncm, $p = .0071$).

4 | DISCUSSION

The present investigation aimed at histometrically comparing the osseointegration and crestal bone healing of two tissue-level implants with a distinctively different endosteal design and bone engagement mechanism resulting in statistically significant different insertion torques and qualitative peri-implant bone healing patterns. The novel tissue-level implant was characterized by a self-cutting tapered endosteal design with a pronouncedly protruding progressive threat geometry. The control was based on conventional and long-term-established predicate tissue-level implants with a long marketing history (van Velzen et al., 2015). Both implant types were further used by strictly adhering to the manufacturer's instructions and hard bone protocols where applicable, resulting in the main experimental variables being the osteotomy preparation and implant design, respectively. Further, it is relevant to mention that both implants machined to microrough surface margins were placed 1 mm subcrestally, which is relevant for interpreting crestal bone healing outcomes.

The applied animal model represents a commonly used and well-established preclinical model to study osseointegration and crestal bone healing in the function of implant design-related aspects with possible relevance to clinical applications (Buser et al., 2004; Mardas et al., 2014; Musskopf et al., 2022). The porcine mandibular bone has been reported to intra- and inter-animal consistently manifest as bone type and density I. Being classified as Misch class D1, this bone displays a thick and dense outer cortical layer with low intrinsic vascularity as compared to more trabecular bone (Misch et al., 1999).

TABLE 1 Bone-to-implant contact—BIC.

Time-point (weeks)	Group	N	Average BIC ± SD (%)	Median BIC (IQR), (%)	BIC range (%)
3	Test	10	73.39 ± 11.12	72.18 (68.18–85.15)	51.65–87.00
	Control	10	71.08 ± 22.18	74.43 (61.945–86.14)	21.365–95.00
6	Test	10	82.08 ± 9.67	83.29 (74.03–89.18)	65.85 –94.66
	Control	9	80.97 ± 9.40	81.16 (78.795–84.46)	67.185–98.55
12	Test	12	81.62 ± 11.12	84.98 (73.43–91.12)	60.73–94.81
	Control	12	90.41 ± 4.81	89.89 (86.20–94.97)	73.43–91.12

Note: Descriptive statistics of histomorphometric-derived bone-to-implant contact (BIC).
Abbreviations: IQR, interquartile range (from first–third quartile); N, sample number, SD, standard deviation.

TABLE 2 First bone-to-implant contact—BIC.

Time-point (weeks)	Group	N	Average fBIC ± S.D., (μm)	Median fBIC (IQR), (μm)	fBIC range, (μm)
3	Test	10	−395.7 ± 251.15	−411.25 (−559 −−135.5)	−769 to −56
	Control	10	−878.6 ± 994.28	−639 (−1273 to −118)	−3212 to −25
6	Test	10	82.08 ± 9.67	83.29 (74.03 –89.18)	65.85–94.66
	Control	9	−369.28 ± 526.60	−112 (−273.5 –to 56.5)	−1312.5 to 0
12	Test	12	−675.58 ± 590.88	−455 (−902 to −313.75)	−2158 to −138
	Control	12	−182.75 ± 197.40	−143.5 (−220 to −18.25)	−609 to 0

Note: Descriptive statistics of histomorphometrically derived first bone-to-implant contact (fBIC).
Abbreviations: IQR: interquartile range (from first–third quartile); N, sample number; SD, standard deviation.

Despite qualitative histological differences in bone engagement and healing and associated different insertion torque values, BIC and fBIC values, except for the 12 weeks' time point, respectively, were noninferior between implants. El Chaar et al. have recently compared the herein-used test and control implants functionalized with a modified hydrophilic surface in a similar model with moderate bone quality (El Chaar et al., 2021). The authors reported lower overall BIC values but similar and noninferior outcomes between test and control implants. Their and other in vitro studies also reported higher maxIT values of the test compared to control implants or implants displaying corresponding endosteal macro designs, respectively (El Chaar et al., 2021; Emmert et al., 2021; Ibrahim et al., 2020).

One of this study's main experimental variables was related to the distinctly different implant macro geometries in conjunction with the corresponding applied osteotomy preparation and placement techniques, i.e., parameters well reported in the literature to influence primary stability and osseointegration (Bilhan et al., 2010; Campos et al., 2012; Cohen et al., 2016; Javed et al., 2013; Marin et al., 2016). Specifically, control implants were placed into diameter and contour-matching osteotomies. In contrast, test implants were placed into parallel-walled osteotomies that were over-contoured with respect to the implants' core diameter and neck and under-contoured with respect to the implant thread dimensions. The placement of self-cutting test implants in as-prepared osteotomies has previously been described to result in cutting, collecting and condensing autologous bone chips in the implant osteotomy (Hadaya et al., 2022). At the same time, the progressive thread design results in apical engagement of the implant with the osteotomy walls, creating healing chambers of apically increasing size

(El Chaar et al., 2021; Marin et al., 2016). Such healing chambers, as evidenced by the qualitative histological examination, were gradually filled over time by de novo bone formation, contributing, next to the resorption and remodeling of bone in primary contact with the implant, to the temporal increase in BIC (Coelho et al., 2010; Jimbo et al., 2014; Marin et al., 2016). Control implants, on the other hand, reached primary stability due to its geometry-matching implant osteotomy. This scenario was previously described to result in bone remodeling and de novo bone formation at the interfacial region as the primary mechanism to generate secondary implant stability (Campos et al., 2012; Jimbo et al., 2014). From this perspective, it may also be interesting to discuss if the different temporal aspects of the two biological mechanisms, i.e. de novo bone formation in healing chambers of test implants compared or resorption and remodeling-based osseointegration of control implants, may have contributed to the observed differences in the temporal evolution of BIC around both implants (Lee & Bance, 2019).

This study also interestingly revealed similar crestal bone levels, except for the 12 weeks outcome, which showed significantly lower fBIC values around control compared to test implants. Previous research has linked the herein applicable study variables, such as the relative implant osteotomy diameter in relation to the implant diameter, over or under-preparation of the associated coronal region, and the specific geometry of the implant collar itself, to influencing the healing and apposition of crestal bone (Abrahamsson & Berglundh, 2006; Campos et al., 2012; Coelho et al., 2010; Heitz-Mayfield et al., 2013; Hermann et al., 2011; Khorsand et al., 2016; Saleh et al., 2018). Moreover, several clinical studies have shown a correlation of high insertion torques values (>50 Ncm) with more
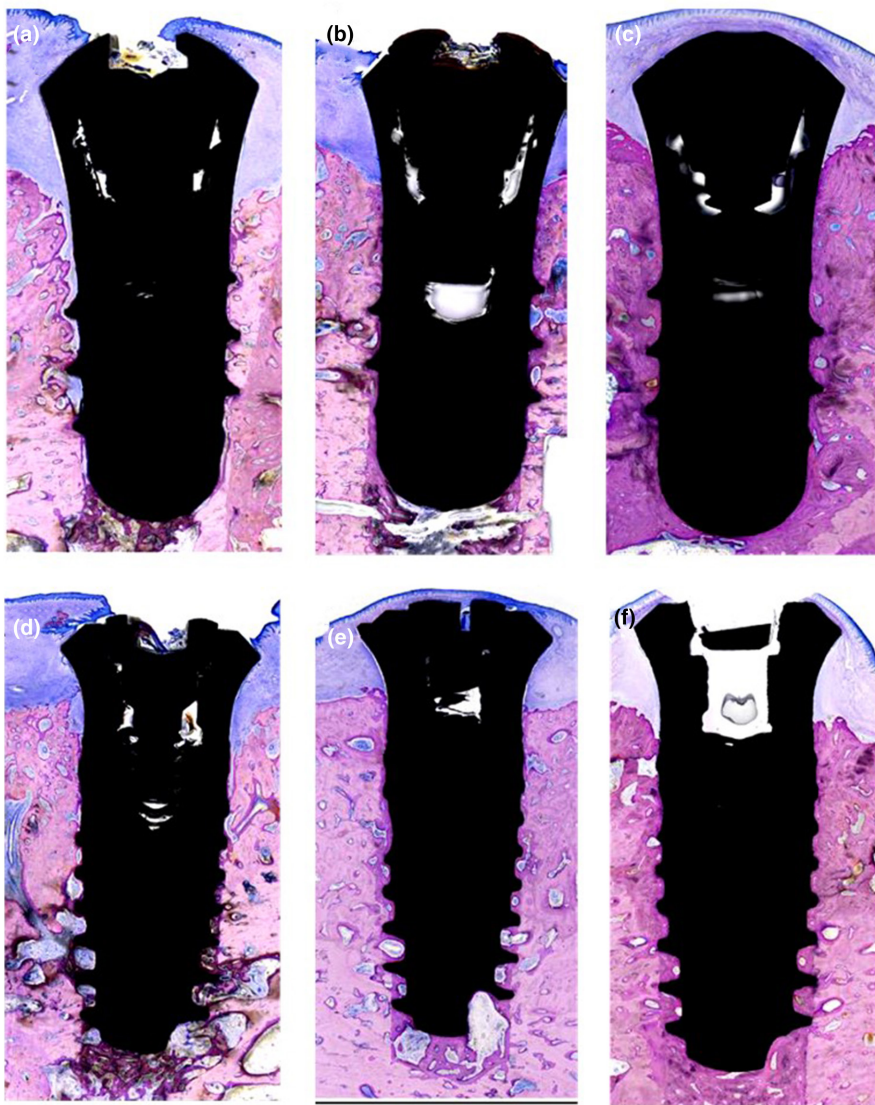
FIGURE 4 Representative histological cross sections illustrating the osseointegration and crestal bone apposition and healing around control implants (a–c) and test implants (d–f) after 3 weeks (a, d), 6 weeks (b, e) and 12 weeks (c, f) of healing.

pronounced crestal bone remodeling (Barone et al., 2016; Oskouei et al., 2023). This, in turn, may have negatively influenced the fBIC values for the test implants at 12 weeks. In contrast, other studies failed to show any difference in terms of crestal bone resorption comparing high and low insertion torques (De Santis et al., 2016; Khayat et al., 2013).

It is important to note that the current study setup comprised a 1 mm subcrestal placement of the rough to smooth surface margin. Botticelli et al. showed that the healing of marginal bone defects around machined surfaces was reduced compared to microrough counterparts (Botticelli et al., 2005). In line with this observation, Hermann et al. have previously shown that subcrestal placement of the rough to smooth surface margin may result in greater bone loss and hence reduced fBIC values compared to equicrestal or supracrestal placement (Hermann et al., 2011). A recent systematic review by Saleh et al. further indicates a potential clinical relevance (Saleh et al., 2018). Consequently, the chosen placement modality may be clearly regarded as unfavourable for crestal bone healing and challenged the implant designs and associated placement modality
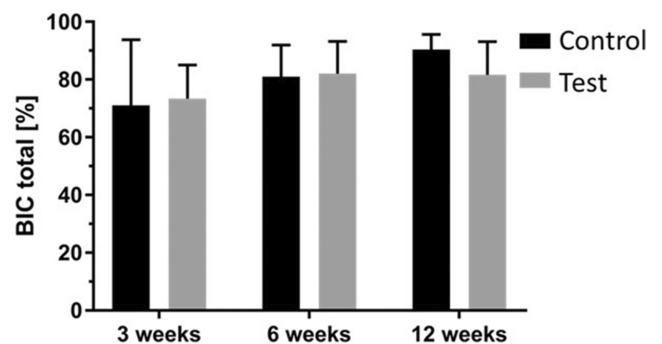
FIGURE 5 Comparison of total BIC values between Control and Test implants after 3, 6, and 12 weeks, respectively. Bars represent mean values, and whiskers represent SD.

regarding their capacity to promote crestal bone healing and apposition within the chosen well-controlled submerged healing regimen.

With test and control implants placed in coronally slightly over-prepared and size-matching osteotomies, respectively, the osteotomy dimensions relative to the implant diameter represented one of the

TABLE 3 Wilcoxon signed rank tests.

Timepoint (weeks)	Outcome	Number of pairs	Mean$_{diff}$ ± SD$_{diff}$	p-value[a]
3	BIC (%)	10	2.314 ± 26.960	.9219
6	BIC (%)	9	0.315 ± 15.367	.9999
12	BIC (%)	12	−8.795 ± 14.286	.1763
3	fBIC (μm)	10	482.9 ± 1087.34	.2324
6	fBIC (μm)	9	−11.388 ± 790.124	.6523
12	fBIC (μm)	12	−492.83 ± 661.895	.0068*

Note: Unadjusted comparisons of BIC and fBIC outcomes per time point as expressed as mean differences between test and control implants. Positive values indicate higher parameters for the test compared to control implants.

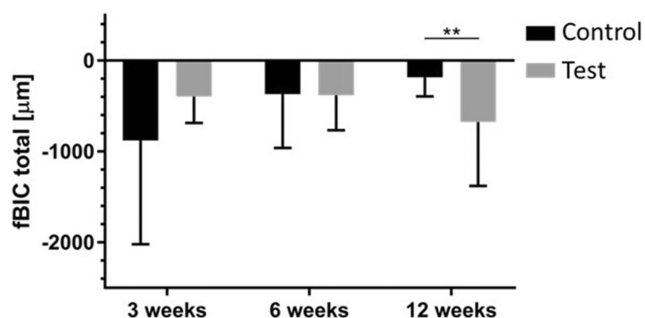[a]p-values were calculated using the Wilcoxon signed rank test (*p < .05).

FIGURE 6 Comparison of mesiodistal averaged first bone-to-implant contacts (fBIC) values between Control and Test implants after 3, 6, and 12 weeks, respectively. Bars represent mean values, and whiskers represent standard deviation. Horizontal bars and asterisks designate compared pairs with statistically significant differences as determined by Wilcoxon signed rank tests paired by implant side and animal: **p ≤ .01.

FIGURE 7 Comparison of primary stability, as determined in the form of averaged maximum insertion torque values (maxIT) between control and test implants. Bars represent mean values, and whiskers represent standard deviation. Horizontal bars and asterisks designate compared pairs with statistically significant differences as determined by Wilcoxon signed rank tests paired by implant site and animal: ** p < .001.

potentially relevant study variables affecting crestal bone apposition. Cortical compression, a previously reported factor to potentially cause crestal bone loss, was absent around both implant types, excluding this aspect as a potential cause for the observed differences between test and control implants (Cohen et al., 2016). Slight coronal overpreparation of osteotomies, within the dimensions of the ones around test implants, on the other hand, have also been previously reported to display a high self-healing tendency (Botticelli et al., 2003; Rossi et al., 2012). Finally, the implant neck geometry represented a study variable between test and control implants, which has repeatedly been reported to influence crestal bone levels (Abrahamsson & Berglundh, 2006; Heitz-Mayfield et al., 2013; Khorsand et al., 2016). An interpretation of the influence of specific implant neck design features of test and control implants is beyond the scope of the current investigation. However, the different and almost diametral temporal evolution of crestal bone levels observed for test and control implants supports the relative importance of this implant design feature as a possible subject for more detailed and dedicated future investigations.

5 | CONCLUSION

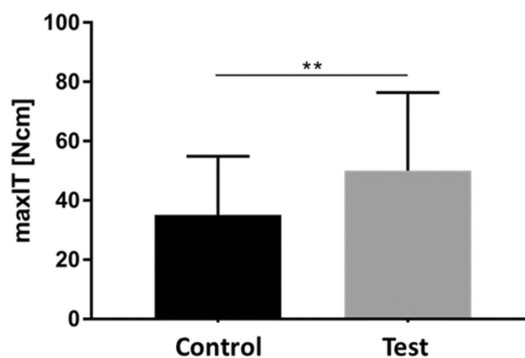Novel microrough self-cutting tissue-level test implants have shown noninferior osseointegrative potential compared to predicate long-term-established tissue-level control implants with equivalent surface functionalization. Crestal bone levels performed comparably in the applied challenging 1 mm subcrestal placement regimen except for the 12 weeks' time point, which resulted in superior outcomes of control compared to test implants. Histometric outcomes between test and control implants in the herein applied model remained noninferior despite significant differences in the basic geometry of the implants and associated differences in insertion torque and qualitative bone healing patterns.

CONFLICT OF INTEREST STATEMENT

The study was founded by Institut Straumann AG. B.P. is an empoyer of the Institut Straumann AG.

The other authors report no conflict of interest related to this study.

DATA AVAILABILITY STATEMENT

The authors confirm that the data supporting the findings of this study are available within the article and its supplementary materials. Further data that support the findings of this study are available from the corresponding author [J.-C.I.], upon reasonable request.

ETHICS STATEMENT

The study protocol was approved by the local ethics committee of the Biomedical Department of Lund University, Lund, Sweden (approval number 2021-15-0201-00876). It respected the Swedish Animal Protection Law, adhered to the ARRIVE Guidelines, and was designed and performed under consideration of the 3R (Replace, Reduce, Refine) guidelines for animal experimentation.

ORCID

Jean-Claude Imber https://orcid.org/0000-0001-6690-5249
Andrea Roccuzzo https://orcid.org/0000-0002-8079-0860
Dieter D. Bosshardt https://orcid.org/0000-0002-2132-6363
Anton Sculean https://orcid.org/0000-0003-2836-5477
Benjamin E. Pippenger https://orcid.org/0000-0001-7990-5555

REFERENCES

Abrahamsson, I., & Berglundh, T. (2006). Tissue characteristics at micro-threaded implants: An experimental study in dogs. *Clinical Implant Dentistry and Related Research*, 8, 107–113.

Barone, A., Alfonsi, F., Derchi, G., Tonelli, P., Toti, P., Marchionni, S., & Covani, U. (2016). The effect of insertion torque on the clinical outcome of single implants: A randomized clinical trial. *Clinical Implant Dentistry and Related Research*, 18, 588–600.

Bilhan, H., Geckili, O., Mumcu, E., Bozdag, E., Sünbüloğlu, E., & Kutay, O. (2010). Influence of surgical technique, implant shape and diameter on the primary stability in cancellous bone. *Journal of Oral Rehabilitation*, 37, 900–907.

Botticelli, D., Berglundh, T., Buser, D., & Lindhe, J. (2003). Appositional bone formation in marginal defects at implants. *Clinical Oral Implants Research*, 14, 1–9.

Botticelli, D., Berglundh, T., Persson, L. G., & Lindhe, J. (2005). Bone regeneration at implants with turned or rough surfaces in self-contained defects. An experimental study in the dog. *Journal of Clinical Periodontology*, 32, 448–455.

Buser, D., Broggini, N., Wieland, M., Schenk, R. K., Denzer, A. J., Cochran, D. L., Hoffmann, B., Lussi, A., & Steinemann, S. G. (2004). Enhanced bone apposition to a chemically modified SLA titanium surface. *Journal of Dental Research*, 83, 529–533.

Campos, F. E., Gomes, J. B., Marin, C., Teixeira, H. S., Suzuki, M., Witek, L., Zanetta-Barbosa, D., & Coelho, P. G. (2012). Effect of drilling dimension on implant placement torque and early osseointegration stages: An experimental study in dogs. *Journal of Oral and Maxillofacial Surgery*, 70, e43–e50.

Chen, S., Wilson, T., & Hämmerle, C. (2004). Immediate or early placement of implants following tooth extraction: Review of biological basis, clinical proceedures, and outcomes. *The International Journal of Oral & Maxillofacial Implants*, 19(Suppl), 12–25.

Cochran, D. L. (2000). The scientific basis for and clinical experiences with Straumann implants including the ITI dental implant system: A consensus report. *Clinical Oral Implants Research*, 11(Suppl 1), 33–58.

Coelho, P. G., Suzuki, M., Guimaraes, M. V. M., Marin, C., Granato, R., Gil, J. N., & Miller, R. J. (2010). Early bone healing around different implant bulk designs and surgical techniques: A study in dogs. *Clinical Implant Dentistry and Related Research*, 12, 202–208.

Cohen, O., Ormianer, Z., Tal, H., Rothamel, D., Weinreb, M., & Moses, O. (2016). Differences in crestal bone-to-implant contact following an under-drilling compared to an over-drilling protocol. A study in the rabbit tibia. *Clinical Oral Investigations*, 20, 2475–2480.

Cosola, S., Marconcini, S., Boccuzzi, M., Fabris, G. B. M., Covani, U., Peñarrocha-Diago, M., & Peñarrocha-Oltra, D. (2020). Radiological outcomes of bone-level and tissue-level dental implants: Systematic review. *International Journal of Environmental Research and Public Health*, 17, 1–22.

De Santis, D., Cucchi, A., Rigoni, G., Longhi, C., & Nocini, P. (2016). Relationship between primary stability and crestal bone loss of implants placed with high insertion torque: A 3-year prospective study. *The International Journal of Oral & Maxillofacial Implants*, 31, 1126–1134.

Duong, H. Y., Roccuzzo, A., Stähli, A., Salvi, G. E., Lang, N. P., & Sculean, A. (2022). Oral health-related quality of life of patients rehabilitated with fixed and removable implant-supported dental prostheses. *Periodontology 2000*, 88, 201–237.

El Chaar, E., Puisys, A., Sabbag, I., Bellón, B., Georgantza, A., Kye, W., & Pippenger, B. E. (2021). A novel fully tapered, self-cutting tissue-level implant: Non-inferiority study in minipigs. *Clinical Oral Investigations*, 25, 6127–6137.

Emmert, M., Gülses, A., Behrens, E., Karayürek, F., Acil, Y., Wiltfang, J., & Spille, J. H. (2021). An experimental study on the effects of the cortical thickness and bone density on initial mechanical anchorage of different Straumann® implant designs. *International Journal of Implant Dentistry*, 7, 83.

Francisco, H., Finelle, G., Bornert, F., Sandgren, R., Herber, V., Warfving, N., & Pippenger, B. E. (2021). Peri-implant bone preservation of a novel, self-cutting, and fully tapered implant in the healed crestal ridge of minipigs: Submerged vs. transgingival healing. *Clinical Oral Investigations*, 25, 6821–6832.

Hadaya, D., Pi-Anfruns, J., Bellon, B., Pippenger, B. E., & Aghaloo, T. L. (2022). Immediate loading of a fully tapered implant with deep apical threads placed in healed alveolar ridges vs. immediate extraction sockets. *Clinical Oral Implants Research*, 33, 501–510.

Heitz-Mayfield, L. J. A., Darby, I., Heitz, F., & Chen, S. (2013). Preservation of crestal bone by implant design. A comparative study in minipigs. *Clinical Oral Implants Research*, 24, 243–249.

Hermann, J. S., Jones, A. A., Bakaeen, L. G., Buser, D., Schoolfield, J. D., & Cochran, D. L. (2011). Influence of a machined collar on crestal bone changes around titanium implants: A histometric study in the canine mandible. *Journal of Periodontology*, 82, 1329–1338.

Hermann, J. S., Schoolfield, J. D., Schenk, R. K., Buser, D., & Cochran, D. L. (2001). Influence of the size of the microgap on crestal bone changes around titanium implants. A histometric evaluation of unloaded non-submerged implants in the canine mandible. *Journal of Periodontology*, 72, 1372–1383.

Ibrahim, A., Heitzer, M., Bock, A., Peters, F., Möhlhenrich, S. C., Hölzle, F., Modabber, A., & Kniha, K. (2020). Relationship between implant geometry and primary stability in different bony defects and variant

bone densities: An in vitro study. *Materials (Basel, Switzerland)*, *13*, 1–16.

Imai, M., Ogino, Y., Tanaka, H., Koyano, K., Ayukawa, Y., & Toyoshima, T. (2022). Primary stability of different implant macrodesigns in a sinus floor elevation simulated model: An ex vivo study. *BMC Oral Health*, *22*(1), 332.

Insua, A., Galindo-Moreno, P., Miron, R. J., Wang, H. L., & Monje, A. (2023). Emerging factors affecting peri-implant bone metabolism. *Periodontology 2000*, *94*(1), 27–78.

Javed, F., Ahmed, H., Crespi, R., & Romanos, G. (2013). Role of primary stability for successful osseointegration of dental implants: Factors of influence and evaluation. *Interventional Medicine & Applied Science*, *5*, 162–167.

Jimbo, R., Tovar, N., Anchieta, R. B., MacHado, L. S., Marin, C., Teixeira, H. S., & Coelho, P. G. (2014). The combined effects of undersized drilling and implant macrogeometry on bone healing around dental implants: An experimental study. *International Journal of Oral and Maxillofacial Surgery*, *43*, 1269–1275.

Kan, J. Y. K., Rungcharassaeng, K., Deflorian, M., Weinstein, T., Wang, H. L., & Testori, T. (2018). Immediate implant placement and provisionalization of maxillary anterior single implants. *Periodontology 2000*, *77*, 197–212.

Khayat, P. G., Arnal, H. M., Tourbah, B. I., & Sennerby, L. (2013). Clinical outcome of dental implants placed with high insertion torques (up to 176 Ncm). *Clinical Implant Dentistry and Related Research*, *15*, 227–233.

Khorsand, A., Rasouli-Ghahroudi, A. A., Naddafpour, N., Shayesteh, Y. S., & Khojasteh, A. (2016). Effect of microthread design on marginal bone level around dental implants placed in fresh extraction sockets. *Implant Dentistry*, *25*, 90–96.

Kim, S., Jung, U. W., Cho, K. S., & Lee, J. S. (2018). Retrospective radiographic observational study of 1692 Straumann tissue-level dental implants over 10 years: I. Implant survival and loss pattern. *Clinical Implant Dentistry and Related Research*, *20*, 860–866.

Lee, J. W. Y., & Bance, M. L. (2019). Physiology of osseointegration. *Otolaryngologic Clinics of North America*, *52*, 231–242.

Mardas, N., Dereka, X., Donos, N., & Dard, M. (2014). Experimental model for bone regeneration in oral and cranio-maxillo-facial surgery. *Journal of Investigative Surgery*, *27*, 32–49.

Marin, C., Bonfante, E., Granato, R., Neiva, R., Gil, L. F., Marão, H. F., Suzuki, M., & Coelho, P. G. (2016). The effect of osteotomy dimension on implant insertion torque, healing mode, and osseointegration indicators: A study in dogs. *Implant Dentistry*, *25*, 739–743.

Misch, C. E., Dietsh-Misch, F., Hoar, J., Beck, G., Hazen, R., & Misch, C. M. (1999). A bone quality-based implant system: First year of prosthetic loading. *The Journal of Oral Implantology*, *25*, 185–197.

Molly, L. (2006). Bone density and primary stability in implant therapy. *Clinical Oral Implants Research*, *17*(Suppl 2), 124–135.

Musskopf, M. L., Stadler, A. F., Wikesjö, U. M. E., & Susin, C. (2022). The minipig intraoral dental implant model: A systematic review and meta-analysis. *PLoS One*, *17*, e0264475.

Oskouei, A. B., Golkar, M., Badkoobeh, A., Jahri, M., Sadeghi, H. M. M., Mohammadikhah, M., Abbasi, K., Tabrizi, R., & Alam, M. (2023). Investigating the effect of insertion torque on marginal bone loss around dental implants. *Journal of Stomatology, Oral and Maxillofacial Surgery*, *124*(6S), 101523.

Parvini, P., Buser, D., Pippenger, B. E., Imber, J. C., Stavropoulos, A., Bellón, B., Jarry, C., & Schwarz, F. (2023). Influence of loading and grafting on hard- and soft-tissue healing at immediately placed implants: An experimental study in minipigs. *Journal of Clinical Periodontology*, *50*, 232–241.

Roccuzzo, A., Imber, J. C., Marruganti, C., Salvi, G. E., Ramieri, G., & Roccuzzo, M. (2022). Clinical outcomes of dental implants in patients with and without history of periodontitis: A 20-year prospective study. *Journal of Clinical Periodontology*, *49*(12), 1346–1356.

Romanos, G. E., Ciornei, G., Jucan, A., Malmstrom, H., & Gupta, B. (2014). In vitro assessment of primary stability of Straumann® implant designs. *Clinical Implant Dentistry and Related Research*, *16*, 89–95.

Rossi, F., Botticelli, D., Pantani, F., Pereira, F. P., Salata, L. A., & Lang, N. P. (2012). Bone healing pattern in surgically created circumferential defects around submerged implants: An experimental study in dog. *Clinical Oral Implants Research*, *23*, 41–48.

Saleh, M. H. A., Ravidà, A., Suárez-López del Amo, F., Lin, G. H., Asa'ad, F., & Wang, H. L. (2018). The effect of implant-abutment junction position on crestal bone loss: A systematic review and meta-analysis. *Clinical Implant Dentistry and Related Research*, *20*, 617–633.

Sasada, Y., & Cochran, D. (2017). Implant-abutment connections: A review of biologic consequences and peri-implantitis implications. *The International Journal of Oral & Maxillofacial Implants*, *32*, 1296–1307.

Schulte, W., Kleineikenscheidt, H., Linder, K., & Schareyka, R. (1978). The Tübingen immediate implant in clinical studies. *Deutsch Zahnärztl Zeitschr*, *33*, 348–359.

Tettamanti, L., Andrisani, C., Bassi, M. A., Vinci, R., Silvestre-Rangil, J., & Tagliabue, A. (2017). Immediate loading implants: Review of the critical aspects. *Oral & Implantology*, *10*, 129–139.

van Velzen, F. J. J., Ofec, R., Schulten, E. A. J. M., & ten Bruggenkate, C. M. (2015). 10-year survival rate and the incidence of peri-implant disease of 374 titanium dental implants with a SLA surface: A prospective cohort study in 177 fully and partially edentulous patients. *Clinical Oral Implants Research*, *26*, 1121–1128.

Wilson, T. G., Miller, R. J., Trushkowsky, R., & Dard, M. (2016). Tapered implants in dentistry: Revitalizing concepts with technology: A review. *Advances in Dental Research*, *28*, 4–9.

Xu, D., Wang, Z., Sun, L., Lin, Z., Wan, L., Li, Y., Lin, X., Peng, W., Zhang, Z., & Gao, Y. (2016). Classification of the root position of the maxillary central incisors and its clinical significance in immediate implant placement. *Implant Dentistry*, *25*, 520–524.

SUPPORTING INFORMATION

Additional supporting information can be found online in the Supporting Information section at the end of this article.

How to cite this article: Imber, J.-C., Khandanpour, A., Roccuzzo, A., Irani, D. R., Bosshardt, D. D., Sculean, A., & Pippenger, B. E. (2024). Comparative osseointegration of hydrophobic tissue-level tapered implants—A preclinical in vivo study. *Clinical Oral Implants Research*, *00*, 1–11. https://doi.org/10.1111/clr.14318